

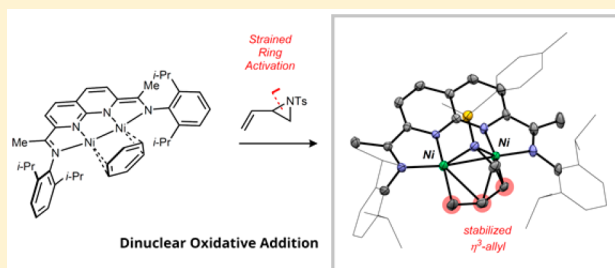
Dinuclear Pathways for the Activation of Strained Three-Membered Rings

Heather R. Rounds, Matthias Zeller, and Christopher Uyeda*[✉]

Department of Chemistry, Purdue University, West Lafayette, Indiana 47907, United States

S Supporting Information

ABSTRACT: Dinuclear, strain-induced ring-opening reactions of vinylaziridines and vinylcyclopropanes are described. The previously reported [NDI]Ni₂(C₆H₆) complex (NDI = naphthyridine–diimine) reacts with *N*-tosyl-2-vinylaziridine via C–N oxidative addition to generate a dinickel metallacyclic product. On the basis of this stoichiometric reactivity, the [NDI]-Ni₂(C₆H₆) complex is shown to be a highly active catalyst for the rearrangement of vinylcyclopropane to cyclopentene. Notably, 2-phenyl-1-vinylcyclopropane undergoes regioselective activation at the less hindered C–C bond in contrast to the noncatalytic thermal rearrangement. DFT calculations provide insight into the ability of the Ni–Ni bond to stabilize key intermediates and transition states along the catalytic pathway.



insight into the ability of the Ni–Ni bond to stabilize key

INTRODUCTION

Cyclopropanes, aziridines, and epoxides participate in a broad range of strain-induced ring-opening reactions mediated by transition metal catalysts.¹ A key step in many of these transformations is a carbon–carbon or carbon–heteroatom oxidative addition that activates the ring and generates a metallacyclic intermediate.² In order to facilitate this process, catalysts that are effective for ring-opening reactions commonly employ strongly donating and sterically encumbering ligands that support electron-rich metals with low coordination numbers (Figure 1).³ For example, Louie demonstrated that (NHC)₂Ni complexes are remarkably active catalysts for the

rearrangement of vinylcyclopropanes to form cyclopentenes.⁴ Computational models suggest that the catalytic intermediates are monoligated Ni species and that C–C oxidative addition is likely rate-determining.⁵

Our group is interested in identifying alternative approaches to promoting bond activation reactions that exploit the cooperative function of multiple metal centers. In this context, we recently described a dinuclear [i-PrNDI]Ni₂(C₆H₆) complex that effects the oxidative addition of allyl chloride to form a Ni₂(μ-allyl)Cl product.⁶ A notable feature of this reaction is its unusually low activation barrier (4.1 kcal/mol by DFT), which we attributed to the ability of the dinuclear system to form a stabilizing π-interaction with the incipient allyl system as the C–Cl bond is cleaved. This observation led us to question whether this activation mode could be generalized to other classes of substrates.⁷ Here, we report a dinuclear mechanism for the stoichiometric and catalytic activation of strained three-membered ring substrates, including vinylaziridines and vinylcyclopropanes.

RESULTS AND DISCUSSION

Stoichiometric Aziridine Ring-Opening. In our initial studies, we examined a stoichiometric oxidative addition reaction of a model strained ring system. Accordingly, [i-PrNDI]Ni₂(C₆H₆) complex **1**⁸ reacts with *N*-tosyl-2-vinylaziridine over the course of 30 min at room temperature to provide the product of C–N oxidative addition (**2**) in 65% isolated yield as a diamagnetic, crystalline green solid (Figure 2a). In a similar fashion to the previously reported [i-PrNDI]-Ni₂(allyl)Cl complex, the solid-state structure features a μ-η³-

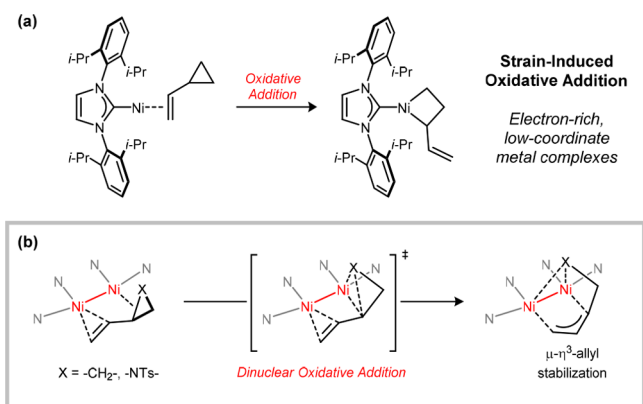


Figure 1. Design principles for strain-induced oxidative addition reactions of vinyl three-membered ring substrates. (a) C–C oxidative addition using electron-rich, low-coordinate metal complexes. (b) Oxidative addition driven by dinuclear stabilization of allyl groups (X = C and N).

Received: December 1, 2017

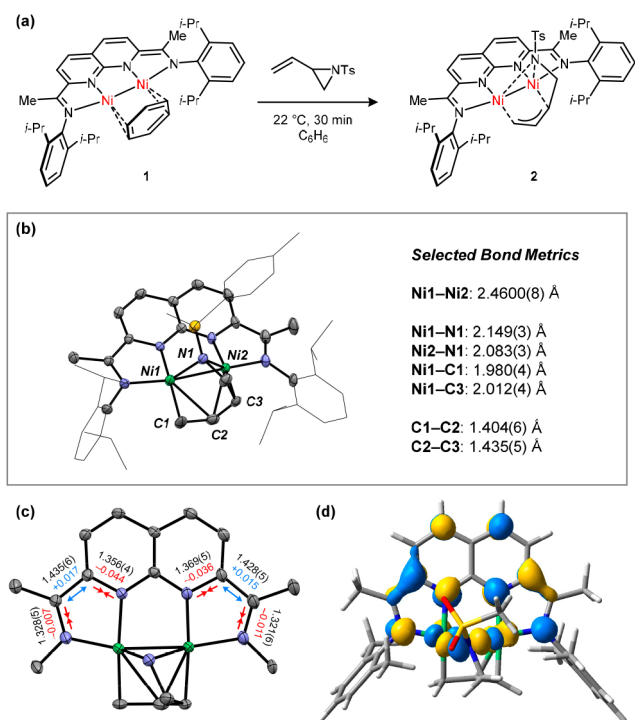


Figure 2. (a) Oxidative addition of *N*-tosyl-2-vinylaziridine using **1**. (b) Solid-state structure for **2** and select bond metrics. (c) Changes in bond metrics indicative of ligand-centered redox activities. Bond metrics for **2** (black) are shown in Å. Changes relative to complex **1** are shown in red and blue. (d) LUMO for **2**, which shows primarily ligand character.

coordination mode for the allyl fragment and a μ -NTs ligand that symmetrically bridges the two metals (Figure 2b). The Ni–Ni bond distance for **2** (2.4600(8) Å) is relatively unchanged from that observed for **1** (2.496(1) Å), suggesting that the electron pair required for the two-electron oxidative addition is being provided by the reduced ligand π -system rather than from the Ni–Ni bond. This description is supported by distortions in the NDI bond metrics that are characteristic of a change in the ligand charge state from dianionic to neutral (Figure 2c). DFT calculations are also consistent with an oxidative addition reaction that involves substantial electronic participation from the redox-active ligand. The calculated LUMO for **2** is predominantly associated with the delocalized NDI π -system with a minor fraction of Ni–Ni π^* character (Figure 2d). This orbital corresponds to the HOMO for Ni₂(C₆H₆) complex **1**.

The [*i*-PrIP]Ni(COD) complex **3** bears a supporting ligand that approximates half of the *i*-Pr⁺NDI system and thus provided a suitable mononuclear analog for **1**. Complex **3** similarly reacts with *N*-tosyl-2-vinylaziridine to yield blue diamagnetic metalacycle **4** in 66% yield (Figure 3a). The ¹H NMR resonances for complex **4** are broad at room temperature but sharpen and resolve at lower temperatures, suggestive of a fluxional process that occurs on the ¹H NMR chemical shift time scale. The most notable structural difference between the dinuclear and mononuclear oxidative addition products is the orientation of the coordinated allyl group (Figure 3b). In **2**, the allyl ligand spans the two Ni centers and is η^3 -coordinated with C1–C2 and C2–C3 distances that are nearly equal. By contrast, the allyl ligand in **4** is η^1 -coordinated, and the C2–C3 distance is

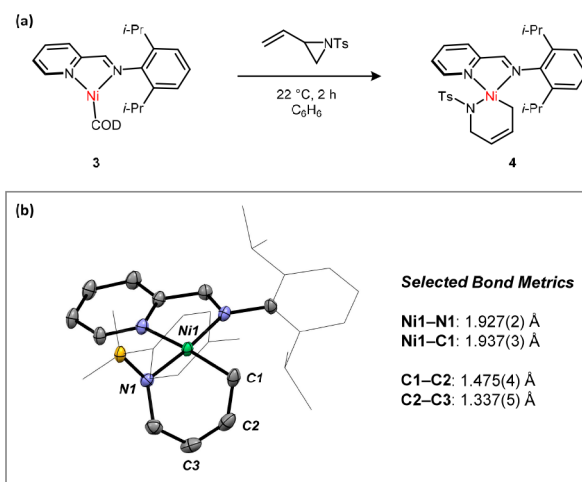
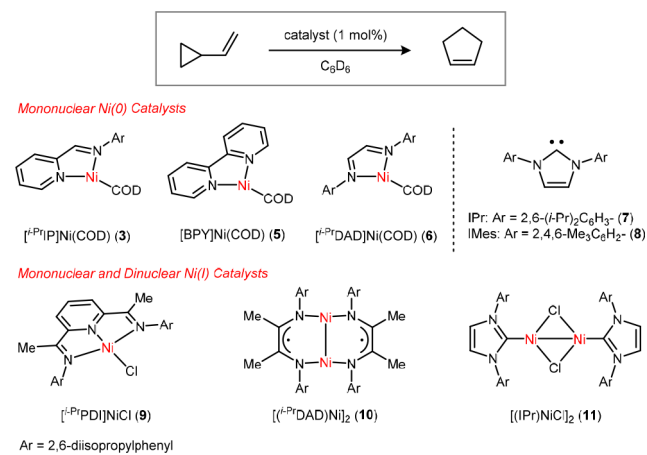


Figure 3. (a) Oxidative addition of *N*-tosyl-2-vinylaziridine using **3**. (b) Solid-state structure for **4** and select bond metrics.

relatively short at 1.337(5) Å, suggesting that it maintains significant double bond character.

Catalytic Rearrangement of Vinylcyclopropane. At 1 mol % loading, [*i*-Pr⁺NDI]Ni₂(C₆H₆) complex **1** catalyzes the rearrangement of vinylcyclopropane to cyclopentene, reaching full conversion after 24 h at room temperature (Table 1). Complex **1** is the only observable catalyst resting state under the reaction conditions. Additionally, in stoichiometric

Table 1. Comparison of Nickel Catalysts for the Rearrangement of Vinylcyclopropane^a



entry	catalyst	time/temp	yield
1	[<i>i</i> -Pr ⁺ NDI]Ni ₂ (C ₆ H ₆) (1)	24 h/22 °C	83%
2	[<i>i</i> -PrIP]Ni(COD) (3)	24 h/60 °C	<1%
3	[BPY]Ni(COD) (5)	24 h/60 °C	<1%
4	[<i>i</i> -Pr ⁺ DAD]Ni(COD) (6)	24 h/60 °C	<1%
5	Ni(COD) ₂	24 h/60 °C	<1%
6	Ni(COD) ₂ + IPr (7) ^b	24 h/60 °C	8%
7	Ni(COD) ₂ + IMes (8) ^b	24 h/60 °C	5%
8	[<i>i</i> -PrPDI]Ni ₂ Cl (9)	24 h/60 °C	<1%
9	[(<i>i</i> -Pr ⁺ DAD)Ni] ₂ (10)	24 h/60 °C	<1%
10	[(IPr)NiCl] ₂ (11)	24 h/22 °C	6%
11	[(IPr)NiCl] ₂ (11)	24 h/60 °C	50%

^aReactions were conducted in a sealed NMR tube, and yields were determined by ¹H NMR integration against a mesitylene standard.

^bConditions: 1 mol % Ni(COD)₂ and 2 mol % NHC.

reactions between **1** and vinylcyclopropane (1.0 equiv), no intermediates are observed en route to cyclopentene, indicating that the catalytic intermediates are endothermic relative to the C_6H_6 adduct.

Mononickel complex **3**, shown above to activate *N*-tosyl-2-vinylaziridine, is not capable of mediating C–C oxidative addition with vinylcyclopropane, providing no detectable conversion of starting material even after 24 h of heating at 60 °C. Related [N,N]Ni(COD) complexes (**5** and **6**) were similarly unreactive under these conditions, as were the mononuclear and dinuclear Ni(I) complexes $[^{i-Pr}PDI]Ni_2Cl$ (**9**)⁹ and $[(^{i-Pr}DAD)Ni]_2$ (**10**).¹⁰ The [NHC]₂Ni catalysts, previously studied by Louie,⁴ are active for the rearrangement of the parent vinylcyclopropane molecule but require elevated temperatures in order to achieve detectable levels of conversion. For example, an IPr/Ni(COD)₂ mixture provides 8% yield of cyclopentene after 24 h of heating at 60 °C. Dimeric [(IPr)NiCl]₂ complex **11**¹¹ is more active than its Ni(0) counterpart, though it is unclear whether **11** might disproportionate under the reaction conditions to generate an active Ni(0) species. It is noteworthy that while the [IPr]₂Ni catalyst is only modestly active for the rearrangement of vinylcyclopropane it is substantially more efficient for substrates bearing alkene substituents.⁴ In contrast, Ni₂ catalyst **1** is only capable of activating substrates with unsubstituted vinyl groups, presumably due to its large steric profile.

For vinylcyclopropane derivatives bearing ring substitutions, the ratio of rearranged cyclopentene isomers is dictated by which of the two cyclopropane C–C bonds is cleaved. In the case of phenyl-substituted vinylcyclopropane **12**, the catalytic rearrangement with **1** selectively targets the less hindered C–C bond, providing **13** in 93% yield as a single isomer (Figure 4).

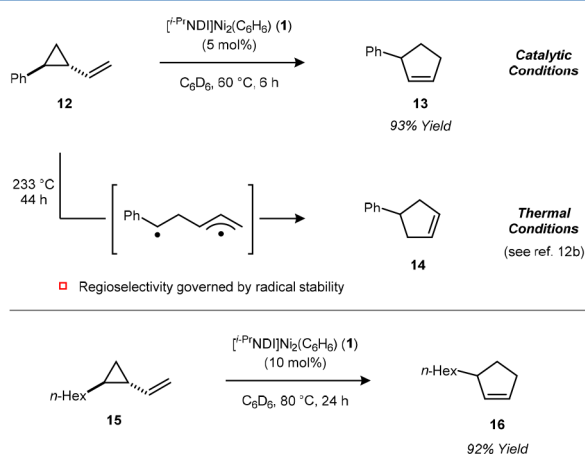


Figure 4. Catalytic rearrangements of vinylcyclopropanes bearing ring substitution.

A similar regioselectivity is observed using the alkyl-substituted vinylcyclopropane **15**, which forms **16** in 92% yield. It is noteworthy that the thermal rearrangement of **12** proceeds at >200 °C and provides only the alternative product isomer **14**.¹² This thermal rearrangement is proposed to occur by C–C bond homolysis to generate a biradical intermediate and is thus governed by the relative stabilities of the benzylic vs the primary radical.

Given the lack of observable intermediates in the Ni₂-catalyzed vinylcyclopropane rearrangement, we turned to DFT models to further probe the mechanism of this reaction (Figure

5). As expected based on our experimental results, the exchange of C_6H_6 for vinylcyclopropane is an endothermic process (+13.7 kcal/mol). The vinylcyclopropane adduct (**B**) exhibits a highly activated C–C bond (1.728 Å), likely due to a strong interaction with the bent C–C σ -bonding orbital of the cyclopropane. Notably, the oxidative addition from **B** is nearly barrierless (<0.1 kcal/mol), and the C–C distance in the transition state (**C**) is elongated by only 0.020 Å relative to **B**. The oxidative addition is highly exothermic and generates a Ni₂ metallacycle (**D**), which closely resembles the analogous structure that was characterized using *N*-tosyl-2-vinylaziridine (Figure 2). From **D**, reductive elimination is calculated to be rate-determining for the catalytic cycle and has an activation energy of 22.1 kcal/mol. Resulting cyclopentene adduct **F** is relatively unstable, and ligand exchange with C_6H_6 to generate the free product is favorable.

It is salient to compare the energetics of the key mechanistic steps using dinuclear catalyst **1** with those previously calculated for the mononuclear [NHC]Ni catalyst.⁵ The most significant consequence of the dinuclear active site is that the oxidative addition transition state and resulting metallacycle intermediate are highly stabilized by the additional π -interactions formed with the second Ni center. The oxidative addition is calculated to be nearly barrierless using **1** but is the rate-determining step for the [NHC]Ni catalyst (approximately 15.6 kcal/mol activation energy).⁵ Likewise, the conversion of the [NHC]Ni vinylcyclopropane adduct to the oxidative addition product is thermoneutral, whereas the analogous dinuclear oxidative addition from **B** to **D** is exothermic by 17.2 kcal/mol using **1**. In contrast to the oxidative addition steps, the C–C reductive elimination is calculated to be more facile for the [NHC]Ni catalyst (15.5 kcal/mol) as compared to that for **1** (22.1 kcal/mol). Overall, these results suggest that dinuclear systems may be particularly suited to accelerating challenging oxidative addition reactions of allylic bonds but do so at the expense of stabilizing the resulting metallacycles and slowing down subsequent reductive elimination.

Catalytic Rearrangements of Heteroatom-Containing Cyclopropanes. We next turned our attention to exploring activation reactions of cyclopropanes bearing pendant heteroatom-containing substituents. Cyclopropyl imine substrate **17** undergoes a catalytic rearrangement with **1** to form acyclic α,β -unsaturated product **18** (Figure 6).¹³ This result suggests that following cyclopropane ring-opening, β -hydride elimination outcompetes the C–N reductive elimination that would lead to 2,5-dihydro-1*H*-pyrrole formation. Similarly, cyclopropylcarboxaldehyde **19** undergoes a catalytic rearrangement to form crotonaldehyde **20** in 80% yield.¹⁴ Finally, cyclopropanol substrate **21** rearranges to ketone **22** in high yield.¹⁵

In summary, the dinuclear active site of the [NDI]Ni₂ platform provides a unique electronic environment for the activation of vinyl-substituted strained rings. The presence of an additional metal center enables precoordination of the alkene and provides stabilization to the allyl system that results from ring opening. Accordingly, oxidative addition reactions of substrates such as vinylaziridines and vinylcyclopropanes proceed with remarkably low activation barriers. Ongoing studies are aimed at exploiting these properties for the activation of other strained and unstrained molecules.

EXPERIMENTAL SECTION

General Information. All manipulations were carried out using standard Schlenk or glovebox techniques under an atmosphere of N₂.

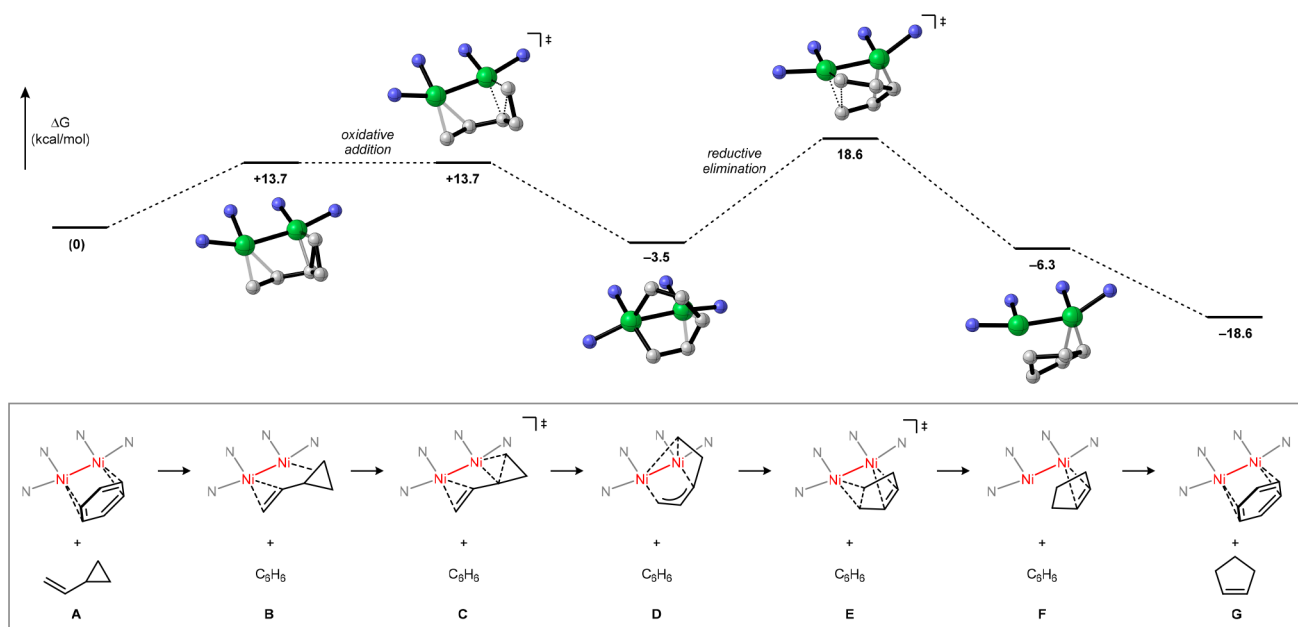


Figure 5. Calculated reaction coordinate for the Ni₂-catalyzed vinylcyclopropane rearrangement (M06/6-31G(d,p) level of DFT). Free energies (ΔG) are in kcal/mol and are relative to that of A. In the model, the catalyst *i*-Pr groups are truncated to Me groups.

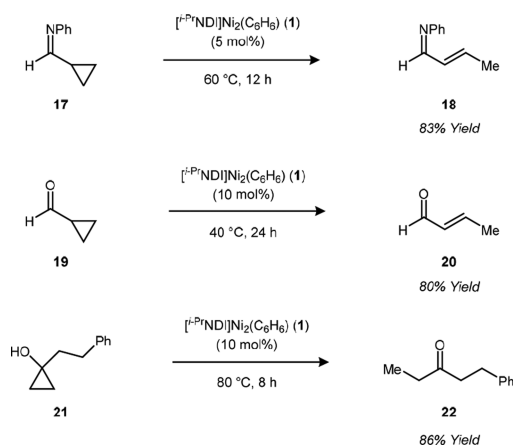


Figure 6. Catalytic rearrangements of cyclopropanes bearing heteroatom-containing substituents.

Solvents were dried and degassed by passing through a column of activated alumina and sparging with Ar gas. Starting materials for the rearrangement reactions were synthesized and purified according to reported procedures. All other reagents were purchased from commercial vendors and used without further purification unless otherwise noted. $[\text{i-PrNDI}]\text{Ni}_2(\text{C}_6\text{H}_6)$ complex **1** was prepared according to previously reported procedures.⁸

Complex 2. In a 20 mL vial, $[\text{i-PrNDI}]\text{Ni}_2(\text{C}_6\text{H}_6)$ (**1**) (30 mg, 0.041 mmol, 1.0 equiv) and 1-tosyl-2-vinylaziridine¹⁶ (9.2 mg, 0.041 mmol, 1.0 equiv) were dissolved in C_6H_6 (5 mL). The solution was observed to undergo an immediate color change from red-brown to green. After stirring at ambient temperature for 30 min, the reaction mixture was filtered through a glass fiber pad, and the filtrate was concentrated to dryness under reduced pressure. The crude residue was washed with pentane (3×1 mL), then dried under reduced pressure to give **2** (21 mg, 65% yield) as a dark green powder. Single crystals suitable for XRD were obtained by cooling saturated solutions of **2** in Et_2O to -30 °C in a glovebox freezer. ^1H NMR (500 MHz, 295 K, C_6D_6) δ 8.79 (br s, 1H), 7.88 (d, $J = 7.4$ Hz, 2H, Ts H), 7.53 (d, $J = 7.5$ Hz, 1H, Ar H), 7.47 (d, $J = 7.5$ Hz, 1H, Ar H), 7.32 (d, $J = 7.0$ Hz, 1H, Ar H), 7.23 (t, $J = 7.7$ Hz, 1H, Ar H), 6.99 (m, 3H), 6.90 (m, 1H), 6.84 (d, $J = 7.5$ Hz, 2H, Ts H), 6.58 (d, $J = 8.0$ Hz, 1H), 6.27 (d, $J = 7.9$ Hz,

1H), 4.96 (d, $J = 6.3$ Hz, 1H), 4.38 (d, $J = 7.5$ Hz, 1H), 3.86 (sept, $J = 11.0$ Hz, 1H, $-\text{CH}(\text{CH}_3)_2$), 3.63 (sept, $J = 7.0$ Hz, 1H, $-\text{CH}(\text{CH}_3)_2$), 3.39 (br s, 1H), 3.35 (d, $J = 11.0$ Hz, 1H), 2.82 (sept, $J = 6.7$ Hz, 1H, $-\text{CH}(\text{CH}_3)_2$), 2.08 (s, 3H, Ts CH_3), 1.67 (s, 6H, imine CH_3), 1.38 (d, $J = 6.6$ Hz, 3H, $-\text{CH}(\text{CH}_3)_2$), 1.29 (d, $J = 6.5$ Hz, 3H, $-\text{CH}(\text{CH}_3)_2$), 1.14 (s, 6H, $-\text{CH}(\text{CH}_3)_2$), 1.03 (d, $J = 6.5$ Hz, 3H, $-\text{CH}(\text{CH}_3)_2$), 0.90 (d, $J = 6.7$ Hz, 3H, $-\text{CH}(\text{CH}_3)_2$), 0.68 (sept, $J = 6.6$ Hz, 1H, $-\text{CH}(\text{CH}_3)_2$), 0.48 (d, $J = 6.7$ Hz, 3H, $-\text{CH}(\text{CH}_3)_2$), 0.23 (d, $J = 6.7$ Hz, 3H, $-\text{CH}(\text{CH}_3)_2$). $^{13}\text{C}\{^1\text{H}\}$ NMR (126 MHz, 295 K, C_6D_6) δ 164.9, 164.4, 162.9, 152.9, 149.3, 147.6, 147.3, 147.3, 146.1, 145.9, 143.9, 141.4, 139.6, 128.8, 128.3, 127.9, 127.7, 127.5, 126.7, 125.9, 124.1, 124.0, 124.0, 123.5, 116.9, 112.4, 108.8, 49.3, 44.8, 29.9, 28.2, 28.0, 27.1, 25.6, 24.8, 24.8, 24.6, 24.3, 24.2, 24.0, 23.8, 21.0, 18.3, 14.5. UV-vis (THF) (λ) $\{\epsilon, \text{cm}^{-1}, \text{M}^{-1}\}$ 667 {4500}, 345 {17 000}, 275 {29 000}. Anal. Calcd for (**2**) ($\text{C}_{47}\text{H}_{57}\text{N}_5\text{Ni}_2\text{O}_2\text{S}$): C 64.63%, H 6.58%, N 8.02%. Found: C 64.85%, H 6.75%, N 7.76%.

Complex 4. In a 20 mL vial, $[\text{i-PrIP}]\text{Ni}(\text{COD})$ (**3**)¹⁷ (40 mg, 0.093 mmol, 1.0 equiv) and 1-tosyl-2-vinylaziridine (21 mg, 0.093 mmol, 1.0 equiv) were dissolved in THF (5 mL). The solution was observed to undergo a gradual color change from purple to blue. After 2 h, the reaction mixture was filtered through a glass fiber pad, and the filtrate was concentrated to dryness under reduced pressure. The crude residue was washed with pentane (3×1 mL), then dried under reduced pressure to give **4** (33.6 mg, 66%) as a dark blue powder. Single crystals suitable for XRD were obtained by cooling saturated solutions of **4** in Et_2O to -30 °C in a glovebox freezer. ^1H NMR (500 MHz, 233 K, toluene- d_8) δ 9.51 (s, 1H, CHNAr), 8.28 (d, 2H, Ar H), 7.61 (s, 1H, Ar H), 6.91 (m, 4H, Ar H), 6.06 (d, $J = 8.5$ Hz, 1H, $\text{CH}=\text{CH}$), 5.22 (d, $J = 8.4$ Hz, 1H, $\text{CH}=\text{CH}$), 4.21 (s, 1H, $-\text{CH}(\text{CH}_3)_2$), 3.80 (d, $J = 16.6$ Hz, 1H, $-\text{CH}(\text{CH}_3)_2$), 3.03–2.90 (m, 2H, $-\text{CH}(\text{CH}_3)_2$), 2.51 (d, $J = 16.8$ Hz, 1H, $-\text{CH}(\text{CH}_3)_2$), 2.22–2.11 (m, 1H), 1.96 (s, 3H, CH_3), 1.58 (d, $J = 5.6$ Hz, 3H, $\text{CH}(\text{CH}_3)_2$), 1.18–1.02 (m, 6H, $-\text{CH}(\text{CH}_3)_2$), 0.76 (d, $J = 5.9$ Hz, 3H, $-\text{CH}(\text{CH}_3)_2$). $^{13}\text{C}\{^1\text{H}\}$ NMR (126 MHz, 295 K, C_6H_6) δ 164.3, 152.2, 145.0, 145.6, 142.2, 140.6, 139.4, 137.2, 131.8, 128.8, 128.6, 128.3, 127.9, 127.7, 127.6, 123.9, 123.4, 47.2, 28.3, 24.5, 22.8, 20.8, 16.8. UV-vis (THF) (λ) $\{\epsilon, \text{cm}^{-1}, \text{M}^{-1}\}$ 329 {1800}, 273 {15 000}, 228 {33 000}. Anal. Calcd for (**4**) ($\text{C}_{29}\text{H}_{35}\text{N}_3\text{NiO}_2\text{S}$): C 63.52%, H 6.43%, N 7.66%. Found: C 63.48%, H 6.39%, N 7.66%.

General Procedure for the Catalytic Rearrangement of Vinylcyclopropane (Table 1). In an N_2 -filled glovebox, vinylcyclopropane⁸ (0.14 mmol), mesitylene (0.14 mmol), and the Ni

catalyst (0.0014 mmol, 1 mol %) were dissolved in C_6D_6 (0.5 mL), and the solution was loaded into an NMR tube equipped with a J. Young valve. The reaction mixture was allowed to react at ambient temperature or 60 °C for 24 h, and the yield of cyclopentene was determined by 1H NMR integration against the mesitylene standard.

Catalytic Rearrangement of 1-Phenyl-2-vinylcyclopropane (12). In an N_2 -filled glovebox, 1-phenyl-2-vinylcyclopropane¹⁹ (29 mg, 0.20 mmol), mesitylene (24 mg, 0.20 mmol), and [^{i-Pr}Ndi] $Ni_2(C_6H_6)$ (7.3 mg, 0.01 mmol, 5 mol %) were dissolved in C_6D_6 (0.5 mL), and the solution was loaded into an NMR tube equipped with a J. Young valve. The reaction mixture was allowed to react at 60 °C for 6 h, and the yield of 3-phenylcyclopentene²⁰ was determined by 1H NMR integration against the mesitylene standard (93% yield). The crude mixture was directly loaded on to a SiO_2 column for purification (mobile phase: pentane). 3-Phenylcyclopentene (13) was isolated in 52% yield (15 mg) as a colorless oil. 1H NMR (500 MHz, 295 K, $CDCl_3$) δ 7.33–7.28 (m, 2H, Ar H), 7.23–7.18 (m, 3H, Ar H), 5.96 (dq, J = 5.7, 2.3 Hz, 1H, $CH=CH$), 5.80 (dq, J = 5.7, 2.1 Hz, 1H, $CH=CH$), 3.91 (m, 1H, CH), 2.58–2.47 (m, 1H, CH_2), 2.47–2.37 (m, 2H, CH_2), 1.79–1.69 (m, 1H, CH_2). $^{13}C\{^1H\}$ NMR (126 MHz, 295 K, $CDCl_3$) δ 146.5, 134.3, 131.9, 128.4, 127.2, 126.0, 51.4, 33.9, 32.5.

Catalytic Rearrangement of 1-Hexyl-2-vinylcyclopropane (15). In an N_2 -filled glovebox, 1-hexyl-2-vinylcyclopropane (15.2 mg, 0.10 mmol), mesitylene (12 mg, 0.10 mmol), and [^{i-Pr}Ndi] $Ni_2(C_6H_6)$ (7.3 mg, 0.01 mmol, 10 mol %) were dissolved in C_6D_6 (0.5 mL), and the solution was loaded into an NMR tube equipped with a J. Young valve. The reaction mixture was allowed to react at 80 °C for 24 h, and the yield of 3-hexylcyclopentene²¹ was determined by 1H NMR integration against the mesitylene standard (92% yield). The crude mixture was directly loaded on to a SiO_2 column for purification (mobile phase: pentane). 3-Hexylcyclopentene (16) was isolated in 58% yield (9 mg) as a colorless oil. 1H NMR (500 MHz, 295 K, $CDCl_3$) δ 5.69 (m, 2H, $CH=CH$), 2.63 (br s, 1H), 2.30 (m, 2H), 2.03 (m, 1H), 1.35 (m, 11H, CH_2), 0.89 (t, J = 6.6 MHz, 3H, CH_3). $^{13}C\{^1H\}$ NMR (126 MHz, 295 K, C_6D_6) δ 135.5, 123.0, 45.6, 36.2, 32.0, 31.9, 29.9, 29.6, 28.0, 22.7, 14.1.

Catalytic Rearrangement of 17. In an N_2 -filled glovebox, 17²² (8.0 mg, 0.054 mmol), mesitylene (6.6 mg, 0.054 mmol), and [^{i-Pr}Ndi] $Ni_2(C_6H_6)$ (2 mg, 0.0027 mmol, 5 mol %) were dissolved in C_6D_6 (0.5 mL), and the solution was loaded into an NMR tube equipped with a J. Young valve. The reaction mixture was allowed to react at 60 °C for 12 h, and the yield of 18 was determined by 1H NMR integration against the mesitylene standard (83% yield). 1H NMR (300 MHz, 295 K, C_6D_6) δ 7.87 (d, J = 8.8 Hz, 1H, $-CHNPh$), 7.25–6.98 (m, 5H, Ar H), 6.64–6.45 (m, 1H, $-CH=CHCH_3$), 5.87 (m, 1H, $-CH=CHCH_3$), 1.49 (d, J = 6.8 Hz, 3H, CH_3).

Catalytic Rearrangement of 19. In an N_2 -filled glovebox, cyclopropanecarboxaldehyde 19 (4.4 mg, 0.063 mmol), mesitylene (7.6 mg, 0.063 mmol), and [^{i-Pr}Ndi] $Ni_2(C_6H_6)$ (5 mg, 0.0063 mmol, 10 mol %) were dissolved in C_6D_6 (0.5 mL), and the solution was loaded into an NMR tube equipped with a J. Young valve. The reaction mixture was allowed to react at 40 °C for 24 h, and the yield of 20 was determined by 1H NMR integration against the mesitylene standard (80% yield). 1H NMR (300 MHz, 295 K, $CDCl_3$) δ 9.27 (d, J = 6.7 Hz, 1H, $-CHO$), 6.03–5.77 (m, 2H, $CH=CH$), 1.30 (d, J = 5.4 Hz, 3H, CH_3).

Catalytic Rearrangement of 21. In an N_2 -filled glovebox, 1-phenethylcyclopropan-1-ol²³ 21 (4.4 mg, 0.027 mmol), mesitylene (3.3 mg, 0.027 mmol), and [^{i-Pr}Ndi] $Ni_2(C_6H_6)$ (2 mg, 0.0027 mmol, 10 mol %) were dissolved in C_6D_6 (0.5 mL), and the solution was loaded into an NMR tube equipped with a J. Young valve. The reaction mixture was allowed to react at 80 °C for 8 h, and the yield of 22²⁴ was determined by 1H NMR integration against the mesitylene standard (86% yield). 1H NMR (400 MHz, 295 K, $CDCl_3$) δ 7.32–7.24 (m, 2H, Ar H), 7.19 (m, 3H, Ar H), 2.90 (t, J = 7.6 Hz, 2H, CH_2), 2.74 (t, J = 7.7 Hz, 2H, CH_2), 2.40 (q, J = 7.3 Hz, 2H, $-CH_2CH_3$), 1.04 (t, J = 7.3 Hz, 3H, $-CH_2CH_3$).

■ ASSOCIATED CONTENT

Supporting Information

The Supporting Information is available free of charge on the ACS Publications website at DOI: 10.1021/acs.organo-
met.7b00862.

Experimental details and characterization data (PDF)

Cartesian coordinates for calculated structures (XYZ)

Accession Codes

CCDC 1588576–1588577 contain the supplementary crystallographic data for this paper. These data can be obtained free of charge via www.ccdc.cam.ac.uk/data_request/cif, or by emailing data_request@ccdc.cam.ac.uk, or by contacting The Cambridge Crystallographic Data Centre, 12 Union Road, Cambridge CB2 1EZ, UK; fax: +44 1223 336033.

■ AUTHOR INFORMATION

Corresponding Author

*E-mail: cuyeda@purdue.edu.

ORCID

Christopher Uyeda: 0000-0001-9396-915X

Notes

The authors declare no competing financial interest.

■ ACKNOWLEDGMENTS

This research was supported by the NSF (CHE-1554787) and by Purdue University. C.U. is an Alfred P. Sloan Research Fellow. X-ray diffraction data were collected using instruments funded by the NSF (DMR-1337296).

■ REFERENCES

- (1) Recent reviews of transition metal catalyzed epoxide, aziridine, and cyclopropane ring-opening reactions: (a) Jun, C.-H. *Chem. Soc. Rev.* **2004**, *33*, 610–618. (b) Lu, B.-L.; Dai, L.; Shi, M. *Chem. Soc. Rev.* **2012**, *41*, 3318–3339. (c) Gao, Y.; Fu, X.-F.; Yu, Z.-X. *Top. Curr. Chem.* **2014**, *346*, 195–232. (d) Tasker, S. Z.; Standley, E. A.; Jamison, T. F. *Nature* **2014**, *509*, 299–309. (e) Huang, C.-Y.; Doyle, A. G. *Chem. Rev.* **2014**, *114*, 8153–8198. (f) Chen, P.-H.; Billett, B. A.; Tsukamoto, T.; Dong, G. *ACS Catal.* **2017**, *7*, 1340–1360.
- (2) (a) Rybtchinski, B.; Milstein, D. *Angew. Chem., Int. Ed.* **1999**, *38*, 870–883. (b) Souillart, L.; Cramer, N. *Chem. Rev.* **2015**, *115*, 9410–9464.
- (3) (a) Tipper, C. F. H. *J. Chem. Soc.* **1955**, 2045–2046. (b) Adams, D. M.; Chatt, J.; Guy, R. G.; Sheppard, N. *J. Chem. Soc.* **1961**, *0*, 738–742. (c) Schlodder, R.; Ibers, J. A.; Lenarda, M.; Graziani, M. *J. Am. Chem. Soc.* **1974**, *96*, 6893–6900. (d) Lin, B. L.; Clough, C. R.; Hillhouse, G. L. *J. Am. Chem. Soc.* **2002**, *124*, 2890–2891. (e) Ney, J. E.; Wolfe, J. P. *J. Am. Chem. Soc.* **2006**, *128*, 15415–15422. (f) Desnoyer, A. N.; Bowes, E. G.; Patrick, B. O.; Love, J. A. *J. Am. Chem. Soc.* **2015**, *137*, 12748–12751.
- (4) Zuo, G.; Louie, J. *Angew. Chem., Int. Ed.* **2004**, *43*, 2277–2279.
- (5) Wang, S. C.; Troast, D. M.; Conda-Sheridan, M.; Zuo, G.; LaGarde, D.; Louie, J.; Tantillo, D. J. *J. Org. Chem.* **2009**, *74*, 7822–7833.
- (6) Behlen, M. J.; Zhou, Y.-Y.; Steiman, T. J.; Pal, S.; Hartline, D. R.; Zeller, M.; Uyeda, C. *Dalton Trans.* **2017**, *46*, 5493–5497.
- (7) Hartline, D. R.; Zeller, M.; Uyeda, C. *J. Am. Chem. Soc.* **2017**, *139*, 13672–13675.
- (8) Zhou, Y.-Y.; Hartline, D. R.; Steiman, T. J.; Fanwick, P. E.; Uyeda, C. *Inorg. Chem.* **2014**, *53*, 11770–11777.
- (9) Manuel, T. D.; Rohde, J.-U. *J. Am. Chem. Soc.* **2009**, *131*, 15582–15583.
- (10) Dong, Q.; Yang, X.-J.; Gong, S.; Luo, Q.; Li, Q.-S.; Su, J.-H.; Zhao, Y.; Wu, B. *Chem. - Eur. J.* **2013**, *19*, 15240–15247.

- (11) Dible, B. R.; Sigman, M. S.; Arif, A. M. *Inorg. Chem.* **2005**, *44*, 3774–3776.
- (12) (a) Marvell, E. N.; Lin, C. *J. Am. Chem. Soc.* **1978**, *100*, 877–883. (b) Baldwin, J. E.; Bonacorsi, S. J. *J. Am. Chem. Soc.* **1996**, *118*, 8258–8265.
- (13) Kamitani, A.; Chatani, N.; Morimoto, T.; Murai, S. *J. Org. Chem.* **2000**, *65*, 9230–9233.
- (14) (a) Ogoshi, S.; Nagata, M.; Kurosawa, H. *J. Am. Chem. Soc.* **2006**, *128*, 5350–5351. (b) Tamaki, T.; Nagata, M.; Ohashi, M.; Ogoshi, S. *Chem. - Eur. J.* **2009**, *15*, 10083–10091.
- (15) (a) Ye, R.; Yuan, B.; Zhao, J.; Ralston, W. T.; Wu, C.-Y.; Unel Barin, E.; Toste, F. D.; Somorjai, G. A. *J. Am. Chem. Soc.* **2016**, *138*, 8533–8537. (b) Okumoto, H.; Jinnai, T.; Shimizu, H.; Harada, Y.; Mishima, H.; Suzuki, A. *Synlett* **2000**, *2000*, 0629–0630.
- (16) Cunha, R. L. O. R.; Diego, D. G.; Simonelli, F.; Comasseto, J. V. *Tetrahedron Lett.* **2005**, *46*, 2539.
- (17) Diercks, R.; Dieck tom, H. *Chem. Ber.* **1985**, *118*, 428–435.
- (18) Fischetti, W.; Heck, R. F. *J. Organomet. Chem.* **1985**, *293*, 391–405.
- (19) Itoh, T.; Matsueda, T.; Shimizu, Y.; Kanai, M. *Chem. - Eur. J.* **2015**, *21*, 15955–15959.
- (20) Chen, Z.; Liang, J.; Yin, J.; Yu, G.-A.; Liu, S. H. *Tetrahedron Lett.* **2013**, *54*, 5785–5787.
- (21) You, H.; Rideau, E.; Sidera, M.; Fletcher, S. P. *Nature* **2015**, *517*, 351.
- (22) Meuer, L. H. P.; Johannes, C. G.; Niel, V.; Pandit, U. K. *Tetrahedron* **1984**, *40*, 5185–5195.
- (23) Rosa, D.; Orellana, A. *Chem. Commun.* **2013**, *49*, 5420–5422.
- (24) Lee, D.-Y.; Hong, B.-S.; Cho, E.-G.; Lee, H.; Jun, C.-H. *J. Am. Chem. Soc.* **2003**, *125*, 6372–6373.